Measuring an Operator's Maneuverability Performance in the Haptic Teleoperation of Multiple Robots

Hyoung Il Son, Lewis L. Chuang, Antonio Franchi, Junsuk Kim, Dongjun Lee, Seong-Whan Lee, Heinrich H. Bülthoff, and Paolo Robuffo Giordano

Abstract— **In this paper, we investigate the maneuverability performance of human teleoperators on multi-robots. First, we propose that maneuverability performance can be assessed by a frequency response function that jointly considers the input force of the operator and the position errors of the multi-robot system that is being maneuvered. Doing so allows us to evaluate maneuverability performance in terms of the human teleoperator's interaction with the controlled system. This allowed us to effectively determine the suitability of different haptic cue algorithms in improving teleoperation maneuverability. Performance metrics based on the human teleoperator's frequency response function indicate that maneuverability performance is best supported by a haptic feedback algorithm which is based on an obstacle avoidance force.**

I. INTRODUCTION

The use of a multi-robot system can, oftentimes, deliver an improvement in the solution quality and completion times of tasks, relative to a single robot system [1], [2]. By exploiting a local synergy among component robots, such a distributed behavior-based approach holds additional advantages, such as higher performance in simultaneous spatial domain coverage, better affordability as compared to a single/bulky system, robustness against single point failures [3]. To date, considerable research efforts have been invested in developing the control design of fully autonomous multi-robot systems. In comparison, it is only in recent years that research has started to address the interaction process between human operators and multi-robots, in particular from a bilateral teleoperation perspective [4], [5], [6].

Multi-robot systems that involve the use of Unmanned Aerial Vehicles (UAVs) have received considerable attention from the research community due to their high motion flexibility and their obvious use-potential in dangerous and/or unaccessible locations (e.g., pesticide-spraying, landscape survey, and surveillance/reconnaissance) [7]. Because of this, it is important to consider the bilateral teleoperation of multiple UAVs and to understand how human control performance can be assessed within this context.

In a previous paper, we proposed a passive teleoperation control scheme that allowed a desirable UAV swarm formation to be maintained, by avoiding obstacles and maintaining system stability [8]. In a related study [9], another bilateral teleoperation controller was described which promoted flexibility in UAV formations, by adjusting the connectivity between UAVs according to their immediate environments. In these studies, we focused on developing a bilateral teleoperation strategy that allowed multiple UAVs to be controlled more efficiently and robustly [8], [9].

The overall performance of a bilateral teleoperation system tends to be highly influenced by the human operator's command. This is especially true in the case of multi-robot systems due to their more complex dynamics and interactions. In addition to visual feedback, accurate commands in teleoperation control can also rely on haptic feedback from a remote site. For example, the availability of the appropriate haptic cue feedback can be shown to heighten the perceptual awareness of the human teleoperator over the remote environment that is inhabited by the multi-robot system [10].

There are several objectives in the bilateral teleoperation of remote vehicles. To begin with, the teleoperator's accurate perception of the remote environment has to be supported in order to avoid collisions between the controlled vehicles and environmental obstacles. As mentioned, the provision of appropriate haptic cue feedback can facilitate this, especially when environmental obstacles are not visually detectable due to the limitations of on-board camera (e.g., restricted field of view (FOV), poor camera resolution, or slow visual update rate) [11], [12]. Next, the operator should be able to accurately control the slave system to move along any desired path. Traditionally, assessments of how this is performed has been described purely in terms of tracking error or deviations of the actual path from the desired path. It is less frequent to consider control efforts of the human operator in this context. Nonetheless, it can be argued that maneuverability performance is considerably enhanced when the same tracking performance can be achieved with less control effort. This is especially true for multi-robot systems which can be expected to require more control effort for effective maneuvering compared to single-robot systems.

Frequency response analysis using transfer functions is a general approach in analyzing performance in the domain of

H. I. Son, L. L. Chuang, A. Franchi, and P. Robuffo Giordano are with the Max Planck Institute for Biological Cybernetics, Spemannstraße 38, 72076 Tübingen, Germany. E-mail: {hyoungil.son, lewis.chuang, antonio.franchi, prg}@tuebingen.mpg.de. Phone: +49-7071-601-218, Fax: +49-7071-601-616.

J. Kim and S.-W. Lee are with the Department of Brain and Cognitive Engineering, Korea University, Anam-dong, Seongbuk-gu, Seoul, 136-713 Korea. E-mail: wowkjs@korea.ac.kr; swlee@image.korea.ac.kr.

D. J. Lee was with the Department of Mechanical, Aerospace & Biomedical Engineering, University of Tennessee, Knoxville, TN 37996 USA; now, with the School of Mechanical and Aerospace Engineering, Seoul National University, Seoul, Korea. E-mail: djlee@utk.edu.

H. H. Bülthoff is with the Max Planck Institute for Biological Cybernetics, Spemannstraße 38, 72076 Tübingen, Germany, and with the Department of Brain and Cognitive Engineering, Korea University, Anam-dong, Seongbuk-gu, Seoul, 136-713 Korea. E-mail: hhb@tuebingen.mpg.de.

bilateral teleoperation (e.g., transparency in [13], and position and force tracking in [14]). Likewise, the relationship between the teleoperator's control effort and maneuvering accuracy can be analyzed in terms of a frequency response function for the evaluation of maneuverability performance. Maneuverability has previously been proposed to be an important measure of the effectiveness of master-slave systems [15]. However, this work focused specifically on the transmission of position and force errors between the master and slave. This was done by taking into account the control effort of the operator, a dynamic model for the environment, and a local controller for the master and slave. Specifically, the operator's control effort was not directly measured in a user study, but was instead simulated based on an impedance model of the human operator and the environment.

This previous study was limited in two regards. First, their indices for the maneuverability do not accurately represent an effect of the operator's force on the maneuverability. The proposed indices are calculated using the human force output of the operator's impedance model. However, using the same human force model to evaluate different bilateral teleoperation systems is questionable, since, in practice, the real human force/impedance will be different depending on the particular teleoperation system. Second, it is generally acknowledged, even in [15], that it is difficult to reliably model the impedances of the human operator and the environment, i.e., the components constituting the operator's control effort. This is because they are likely to vary nonlinearly over time as well as across different situations. In light of this, it is preferable to evaluate bilateral teleoperation systems with direct measurements of human behavior, by, e.g., exploiting suitable force sensors placed at the master side.

The objectives of the current study are two-fold: first, we propose that maneuverability performance of multi-robot systems can be evaluated in terms of a frequency response function that jointly considers the maneuvering accuracy and the control efforts of the human teleoperator. Second, we report a psychophysical study that employed this approach in evaluating three candidate algorithms for haptic feedback cues with regards to their role in enhancing maneuverability performance during bilateral teleoperation. These algorithms are based on the UAVs' 1) velocity information, 2) proximity to obstacles in their remote environments, and 3) a combination of these two sources of information.

The structure of this paper is as follows. First, a concept of the maneuverability is presented and metrics for it are defined in Sec. II Following this, we review our previous framework for the haptic teleoperation of multiple UAVs and three haptic feedback algorithms. Finally, we provide a psychophysical evaluation of these haptic feedback algorithms, using our recommended metrics, to determine the algorithm that achieves the best level of maneuverability.

II. MANEUVERABILITY

A. Position Tracking in Time Domain

In conventional teleoperation research, the position tracking ability of the slave is typically evaluated by estimating the discrepancy between the position of the slave and the master. In the current work, we are concerned with the discrepancy between the position of the slave and a reference position on the path that the teleoperator intends to maneuver. Therefore, position tracking error is defined as $e(t) := \bar{x}(t) - x_{ref}(t)$ for N slave robots, where $\bar{x}(t) = \frac{1}{N}\sum_{i=1}^{N} x_i(t)$, $x_i(t) \in \Re^3$ being the position of i^{th} robot, and $x_{ref}(t) \in \Re^3$ being the position on the reference path, at time t. In the conventional teleoperation case, x_{ref} would be replaced by the position of the master x_m.

This position tracking error can be quantitatively evaluated across overall operation time by using cross-correlation (CC) to objectively compare the similarity of the actual path ($\bar{x}$) and the desired path (x_{ref}) of the slave robots. In the current study, we define this cross-correlation as in (1) to estimate the position tracking error across the overall time of maneuvering (T).

$$CC_{position} = \frac{\int_0^T \bar{x}(t) \cdot x_{ref}(t)dt}{\sqrt{\int_0^T \bar{x}^2(t)dt}\sqrt{\int_0^T {x_{ref}}^2(t)dt}} \tag{1}$$

B. Maneuverability in Frequency Domain

As stated previously, maneuverability performance should take into account the control effort of the operator. From the operator's perspective, it is desirable to achieve equivalent maneuvering accuracy with less control effort during bilateral teleoperation. However, the position tracking metric CC does not consider this. From this perspective, we propose that *maneuverability* can be assessed in terms of the ease of the operator in maneuvering the slave robot for achieving accurate tracking performance.

This can be formally defined as the frequency response of the intended-force from the human operator as the input, and the position tracking CC as the output

$$\Phi_{maneuv}(s) := \frac{CC_{position}(s)}{f_h(s)} \tag{2}$$

where $f_h \in \Re^3$ is the intended-force input from the human. The magnitude of the maneuverability becomes large if f_h is small and if the position tracking CC is large (i.e., the position tracking error is small).

From this, two additional performance metrics can be derived for maneuverability. First, the ± 3 dB bandwidth of Φ_{maneuv}, denoted with ω_{bd}. Second, the H_2 norm of Φ_{maneuv}, denoted with $\|\Phi_{maneuv}\|_2$ and defined in (3)

$$\|\Phi_{maneuv}\|_2 = \left\| W_{low}\frac{CC_{position}}{f_h} \right\|_2 \tag{3}$$

where W_{low} is a low-pass weighting function with a cut-off frequency ω_c. We note that the selection of ω_c depends on the specific application of bilateral teleoperation systems.

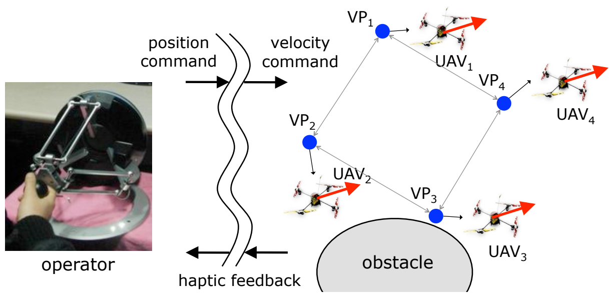

Fig. 1. Haptic teleoperation of multiple UAVs.

As the normal tremor of a human hand occurs at $8 \sim 12$ Hz [16], ω_c can be less than 8 Hz.

The bandwidth and H_2 norm are useful properties of the system, which respectively denote how well the system will track an input and the degree of sensitivity of system output with respect to its input. Thus, large values of ω_{bd} and $\|\Phi_{maneuv}\|_2$ indicate high maneuverability performance.

III. TELEOPERATION OF MULTI-UAVS WITH HAPTIC FEEDBACK

A. Teleoperation Control Architecture

The architecture proposed in [8] for teleoperating multiple UAVs consists of three control layers (see Fig. 1): 1) UAV control layer, where each UAV is controlled to follow the trajectory of an abstract kinematic virtual point (VP); 2) VP control layer, which modulates each VP's motion according to the teleoperation commands and local artificial potentials (for inter-VP/VP-obstacle collision avoidance and inter-VP connectivity preservation); and 3) teleoperation layer, through which a remote human user can command all (or some) of the VPs' velocity while haptically perceiving the state of all (or some) of the UAVs over the Internet. Hereafter, we briefly review these layers and refer the reader to [8] for further details.

1) UAV control layer: We consider N quadrotor-type unmanned aerial vehicles (UAVs), each with under-actuated Lagrangian dynamics in $SE(3)$ [17]. The Cartesian position of each UAV is represented as $x_i \in \Re^3$ is w.r.t. the NED (north-east-down) inertial frame. The quadrotors are endowed with an attitude controller which is able to track a desired trajectory in $\Re^3$, specified by the VP control layer.

2) VP control layer: We implement the following kinematic evolution of the i-th VP p_i on each UAV:

$$\dot{p}_i(t) := u_i^c + u_i^o + u_i^t \tag{4}$$

where

- $u_i^c \in \Re^3$ embeds the inter-VP collision avoidance and connectivity preservation actions;
- $u_i^o \in \Re^3$ represents an obstacle avoidance control;
- $u_i^t \in \Re^3$ is the teleoperation control from a remote human operator for a (non empty) subset $\mathcal{N}_t \subset \{1, 2, ..., N\}$ among the N VPs, to tele-drive the Cartesian velocity of the N VPs network over the Internet. This will be better defined in the next subsection.

3) Teleoperation layer: We consider a 3-degree-of-freedom (DOF) haptic device as modeled by

$$M(q)\ddot{q} + C(q, \dot{q})\dot{q} = \tau + f_h \tag{5}$$

where $q \in \Re^3$ is the configuration, $M(q) \in \Re^{3\times3}$ is the positive-definite/symmetric inertia matrix, $C(q, \dot{q}) \in \Re^{3\times3}$ is the Coriolis matrix, and $\tau, f_h \in \Re^3$ are the control input and human operation forces, respectively.

First, to enable a remote human user to tele-control the VPs/UAVs, we define u_i^t in (4) as

$$u_i^t(t) := \lambda q(t), \quad \forall i \in \mathcal{N}_t \tag{6}$$

where $q(t)$ is the master position $q(t) \in \Re^3$ received via the Internet, and $\lambda > 0$ is to match different scales between $q(t)$ and $\dot{p}_i$. This control enables the user to tele-control the VPs' velocities $\dot{p}_i$ via the master device position $q(t)$.

On the other hand, to enable the user to tele-sense all the VPs/UAVs collectively, we design the haptic feedback signal $y(t) \in \Re^3$ to be sent to the master as a function of the UAV's velocity and the VP's obstacle avoidance control

$$f : (\dot{x}_i, u_i^o) \mapsto y(t) \tag{7}$$

where $\dot{x}_i$ is the UAV's velocity, and u_i^o is the VP's obstacle avoidance control.

This $y(t)$ is then sent to the master over the Internet. Let us denote by $y(k)$ its reception by the master side over the Internet at the (master) reception time t_k. We incorporate this $y(k)$ into the teleoperation control τ as a function of the position and the velocity of the haptic device and the haptic feedback signal in (5) s.t.

$$f : (q, \dot{q}, \bar{y}(k)) \mapsto \tau(t) \tag{8}$$

for $t \in [t_k, t_{k+1})$, where $\bar{y}(k)$ is the passive set-position modulation (PSPM [18]) of $y(k)$. The use of the PSPM algorithm in modulating $y(k)$ allows us to enforce passivity of the master side regardless of time delays and sparse/discrete sampling in receiving $y(t)$.

B. Haptic Feedback Algorithms

We propose three haptic feedback algorithms using 1) the velocity information of UAVs, 2) an obstacle avoidance force, and 3) a combination of the velocity information of UAVs and obstacle avoidance force previously described in [10]. For each of these algorithms, we designed $y(t)$ and $\tau(t)$ in (7) and (8) in the following fashion.

1) Velocity cue: The haptic feedback signal $y(t)$ is designed as

$$y(t) = \frac{1}{\lambda N} \sum \dot{x}_i \tag{9}$$

to transmit the velocity information of the UAVs as a haptic cue. The corresponding teleoperation control $\tau(t)$ is then

$$\tau(t) = -B\dot{q} - K[q - \bar{y}(k)] \tag{10}$$

where $B, K \in \Re^{3\times3}$ are the positive definite and symmetric damping and spring matrices.

This feedback allows the human operator to directly perceive the 'inertia' of the UAVs expressed in (9). Furthermore, the haptic feedback will also inform, in an indirect way, about presence of obstacles. Indeed, an obstacle obstructing the UAV motion will induce an increase in the tracking error between $\dot{p}_i$ and $\dot{x}_i$. The human will then perceive a strong haptic feedback when maneuvering the UAVs toward the obstacles. In addition, this feedback will also inform about disturbances/restrictions of the motion which are not measured by an obstacle detector and hence are not conveyed by u_i^o (e.g., wind gusts, actuation non-idealities).

This haptic feedback algorithm is derived from the well-known position-position (PP) control, also referred to as the position error feedback control, in conventional teleoperation research [19]. However, it should be noted that the control that is currently proposed is a position-velocity control, as evident from (6).

2) Force cue: This cue is defined by

$$y(t) = \frac{1}{\lambda N} \sum u_i^o, \tag{11}$$

$$\tau(t) = -B\dot{q} - K\bar{y}(k). \tag{12}$$

With this haptic feedback algorithm, a force will be fed back to the human only when an obstacle is detected. This algorithm is based on the conventional force-position (FP) control [19], also referred to as the direct force feedback control, which is generally regarded to show better performance than the PP control, but less stability robustness. However, unlike the conventional FP control, our Force cue includes a damping term in (12) that allows to maintain a level of stability robustness, equivalently to the other proposed haptic feedbacks. This additional term can possibly decrease the overall performance due to well-known tradeoffs between the performance and the stability in teleoperation systems.

3) Velocity+Force cue: Finally, a combination of the velocity information of UAVs and the obstacle avoidance force can be transmitted with

$$y(t) = \frac{1}{\lambda N} \sum (\dot{x}_i + u_i^o), \tag{13}$$

$$\tau(t) = -B\dot{q} - K[q - \bar{y}(k)] \tag{14}$$

to the human operator. In the absence of obstacles, this haptic feedback algorithm ought to be equivalent to the *Velocity* cue. However, more haptic force feedback should be experienced by the operator when obstacles are present compared to the separate cues of *Velocity* and *Force*.

From hereafter, these three haptic feedback algorithms will be referred to as *Velocity*, *Force*, and *Velocity+Force* algorithms while their conventional counterparts will be respectively referred to as the PP, FP, and PFP controllers.

IV. PSYCHOPHYSICAL EVALUATION OF HAPTIC FEEDBACK ALGORITHMS

It is not clear which of the proposed three haptic feedback algorithms (i.e., *Velocity*, *Force*, and *Velocity+Force*) are likely to yield haptic cues that will best support maneuverability performance in (1)–(3). Although it has been previously claimed that maneuverability performance is better

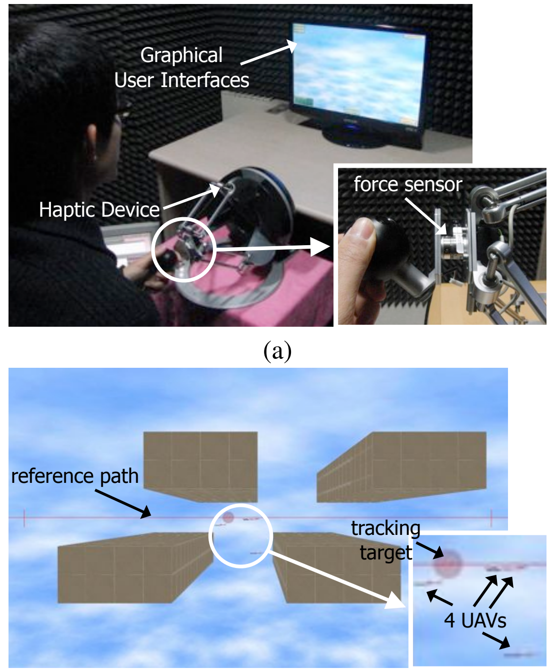

(a)

(b)

Fig. 2. Experimental setup. (a) Subject with haptic device (Omega 3) and Graphical User Interfaces (GUIs). (b) Screen shot with visible reference path and obstacles, which were rendered invisible during the actual experiment.

supported by the PP control scheme, this evaluation was performed with a simulated human force input which was the same for all tested control scheme [15]. Theoretically, it is known that the PP controller delivers position tracking performance comparable to the FP controller in free motion [14], [19]. On the other hand, FP control architecture shows in general better performance than the PP controller in force tracking but has less stability robustness in contact motion [19]. Therefore, we conducted a human psychophysical experiment to evaluate our haptic cue algorithms for how well they supported maneuverability performance in three different bilateral teleoperation scenarios.

A. Participants

Eighteen students (14 males; age range: 25-30 years) of Korea University, Seoul participated in this experiment. All participants were naive to the experiment and apparatus. They possessed normal or corrected-to-normal eyesight and possessed no physical disability. The experiment was conducted in accordance with the requirement of the Helsinki Declaration.

B. Apparatus

The apparatus consisted mainly of a display that presented a virtual environment for a swarm of UAVs and a haptic device that could be used to control the flight path of these UAVs (see Fig. 2(a)).

The UAV swarm always assumed a tetrahedron formation in this virtual environment, with an inter-UAV distance of approximately 0.8 m. The UAVs dynamics and control logic were simulated in a custom-made simulation environment that was based on the Ogre3D engine (for 3D rendering and computational geometry computations), with PhysX libraries to simulate the physical interaction between the UAVs and the environment. The simulation was updated at 60 Hz and this constrained the data exchange rate between the haptic device and virtual UAVs. In the display, the simulated UAVs and environment were rendered from a camera perspective that was 32 m away from the starting positions of the UAVs, with FOV of about 21°. This rendered scene was presented via a display monitor and is depicted in Fig. 2(b).

The UAV swarm was controlled by a commercial haptic device (Omega 3, Force Dimension). The Omega 3 is a 3-DOFs haptic device with 3 translational actuated axes and a local control loop running at about 2.5 kHz on a dedicated linux machine. In addition, ATI six-axis force/torque sensors, Nano17, were attached to the Omega 3 device to measure the force that was exerted on the device by the human operator during the experiment as shown in Fig. 2(a).

C. Procedure

In this experiment, participants were required to maneuver a swarm of UAVs using the haptic control device, in order to follow a reference path defined by a moving target. The moving target preceded the UAV swarm and moved along a path that was either straight or curved. The position and velocity profiles of this tracking target are described by Fig. 3 for both paths. S-shaped velocity profiles were implemented in the acceleration and deceleration phases of the target's motion to allow the operator to track the target better, especially at the beginning of each trial. Prior to experimentation, participants were briefed and given a practice session.

The full experiment was separated into three blocks of 25 trials each. Each block of trials was defined by the type of haptic cue which was provided to the participant; namely, *Velocity*, *Force*, and *Velocity+Force*. The following control parameters (gains) were fixed for the purpose of this experiment: K=70N/m and B=2Ns/m for all haptic cues. This way, the produced force of the *Velocity* cue was comparable with the force of the *Force* cue, and less than the one generated by the *Velocity+Force* cue algorithm. Finally, the presentation order of the blocks was fully counter-balanced across the participants, to minimize the influence of practice and order effects on our findings.

On each trial, participants could be presented one of three possible scenarios for UAVs maneuvering. First, participants could be presented with a scenario that required the UAV swarm to be maneuvered in a straight path, in an environment that contained no obstacles (5 trials). Alternatively, they could be expected to do the same, but in an environment that contained an arrangement of four obstacles, which bounded the straight path as depicted in Fig. 4(a) or (b) (10 trials which is 5 trials times 2 cases). Finally, they could be required to maneuver the UAV swarm in a curved path, which was bounded by an arrangement of four obstacles as is depicted in Fig. 4(c) or (d) (10 trials). The arrangement

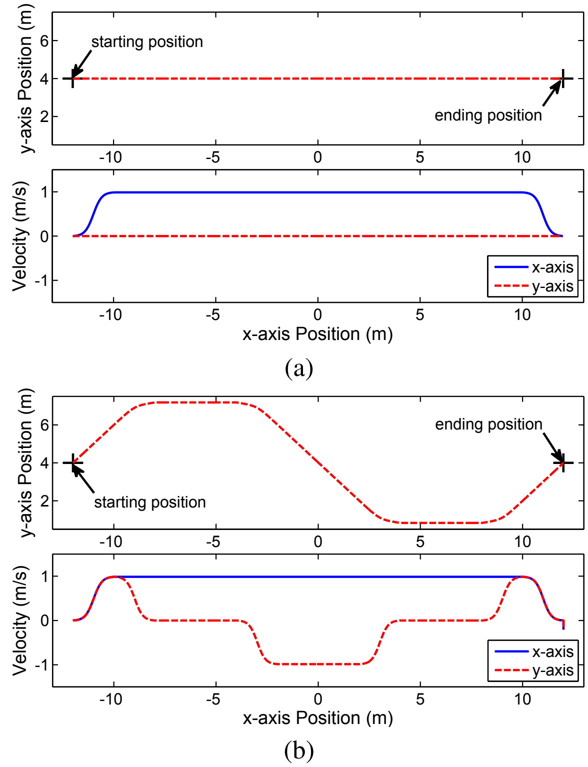

Fig. 3. Position and velocity profiles of the tracking target, when the participant was required to perform a: (a) straight path maneuver, (b) curved path maneuver.

of obstacles, when they were present, was counter-balanced across the relevant experimental trials. These three scenarios featured in all of the blocks and were fully randomized for their presentation order.

Note that the obstacles as well as the reference path were invisible during the experiment to minimize any influence of visual feedback. Only the UAVs and tracking targets were visible during the experiment.

D. Data Analysis

Three measures served as performance metrics for maneuverability in our evaluation study, according to our description in Sec. II. To recap, $CC_{position}(\%)$ represents the similarity between the desired path and the path that was executed by the operator in a percentage, while $\|\Phi_{maneuv}\|_2$ and ω_{bd} represents the H_2 norm and bandwidth of the maneuverability frequency response (Φ_{maneuv}). These measures were separately computed for the x-axis and y-axis components of the maneuvered path. In fact, the dynamics of the quadrotors along y-axis are faster than the x-axis for mechanical reasons. Altogether, this resulted in six performance metrics.

In our study, Φ_{maneuv} was measured as the experimental frequency response of the haptic teleoperation system of multi-UAVs shown in Fig. 2. This considered as input the human operational force to the haptic device (f_h), calculated as

$$f_h(t) = f_m(t) - \tau(t) \tag{15}$$

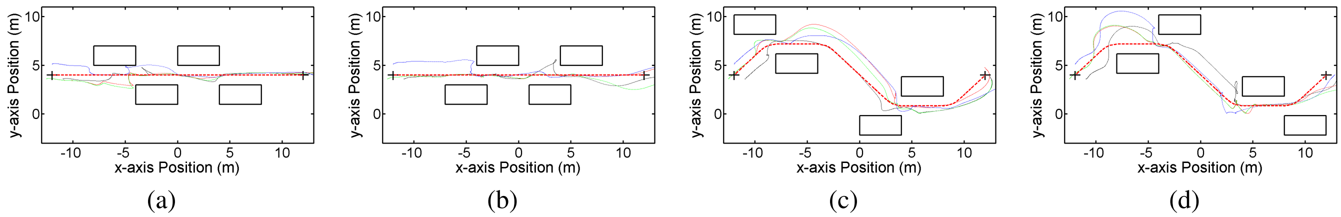

Fig. 4. Configuration of obstacles for: the straight path maneuver (Scenario 2), Case 1 (a), Case 2 (b); the curved path maneuver (Scenario 3) Case 1 (c), Case 2 (d). The dotted red line indicates the ideal path travelled by the tracking target. Other lines represent four examples of paths that were taken by controlled UAV swarms, in the experiment.

where f_m is the force that was measured from the force sensor on the haptic device and τ is the master control force given by the current haptic feedback algorithm. The output is $CC_{position}$ treated in percentage (see (1)). With both variables, it was possible to calculate $\Phi_{maneuv}(s)$ by applying the empirical transfer function estimator (ETFE [20]), using a second-order low-pass filter (W_{low}) with cut-off frequency of 8 Hz (See (3)).

All performance metrics were submitted to a one-way repeated-measures analysis of variance (ANOVA) for the factor of haptic feedback algorithm (*Velocity*, *Force*, and *Velocity+Force*). Performance on the three different scenarios were independently analyzed and are separately reported in the following sub-sections.

An alpha level of 0.05 was taken to indicate statistical significance. When a main effect was found, post-hoc t-tests[1] were conducted among the haptic feedback algorithm conditions to identify those which were significantly different from each other in terms of the relevant performance metrics.

E. Results

1) Scenario 1: Straight path with no obstacles: $\|\Phi_{maneuv}\|_2$ of the x-axis component was the only performance metric that yielded a significant main effect ($F_{2,34} = 24.3, p < 0.001$). Specifically, *Force* resulted in better performance than both *Velocity* and *Velocity+Force* (see Fig. 5(c)).

In comparison, neither $CC_{position}(\%)$ nor ω_{bd} of the x-axis component produced statistically significant results ($CC_{position}(\%)$: $F_{2,34} = 2.3, p = 0.12$; ω_{bd}: $F_{2,34} = 0.87, p = 0.43$).

None of the performance metrics for the y-axis component produced statistically significant results ($CC_{position}(\%)$: $F_{2,34} = 0.32, p = 0.73$; ω_{bd}: $F_{2,34} = 1.03, p = 0.37$; $\|\Phi_{maneuv}\|_2$: $F_{2,34} = 1.19, p = 0.32$). This was expected as the desired path for maneuvering only involved translations along the horizontal x-axis.

2) Scenario 2: Straight path with obstacles: With regards to the x-axis component, maneuverability performance was statistically different across the haptic cues for the performance metrics of $CC_{position}(\%)$ ($F_{2,34} = 5.52, p < 0.01$) and $\|\Phi_{maneuv}\|_2$ ($F_{1.4,23.9} = 61.1, p < 0.001$[2]). With regards to $CC_{position}(\%)$, the post-hoc analyses only revealed a significant difference between *Velocity+Force* and *Velocity* cue (See Fig. 6(a)); performance in terms of $CC_{position}(\%)$ was not significantly different between the *Force* cue and the others, in spite of apparent plotted differences. For $\|\Phi_{maneuv}\|_2$, best performance was achieved with the application of the *Force* cue, relative to both *Velocity* and *Velocity+Force* cues (see Fig. 6(c)).

With regards to the y-axis component, $\|\Phi_{maneuv}\|_2$ was the only performance metric that was statistically different across the three haptic cues ($F_{1.9,34} = 10.1, p < 0.001$). In this regard, the application of the *Force* cue produced the best performance, relative to both *Velocity* and *Velocity+Force* cues (See Fig. 6(c)).

Finally, the performance metric of ω_{bd} did not yield any statistically significant differences, for both the x-axis ($F_{2,34} = 1.36, p = 0.27$) as well as the y-axis component ($F_{2,34} = 1.10, p = 0.34$). However we can appreciate the faster responsiveness (higher bandwidth) of the UAVs along the y-axis, as expected.

3) Scenario 3: Curved path with obstacles: With regards to the x-axis component, there were statistically significant main effects on the performance metrics of $CC_{position}(\%)$ ($F_{1.4,24.4} = 6.6, p < 0.05$) and $\|\Phi_{maneuv}\|_2$ ($F_{2,34} = 22.8, p < 0.001$). The same results were found for the y-axis component ($CC_{position}(\%)$: $F_{1.5,25.4} = 6.49, p < 0.01$; $\|\Phi_{maneuv}\|_2$: $F_{2,34} = 46.8, p < 0.001$).

In both cases, the post-hoc analyses produced the same pattern of results. For $CC_{position}(\%)$, performance with the *Velocity+Force* cue was worse than the *Velocity* cue. Performance with the *Force* cue was not statistically different to performance with *Velocity* and *Velocity+Force* cues (See Fig. 7(a)). There was no significant difference between the *Velocity* and *Force* cues. For $\|\Phi_{maneuv}\|_2$, best performance was achieved with the application of the *Force* cue, relative to both *Velocity* and *Velocity+Force* cues (see Fig. 7(c)).

Finally, the performance metric of ω_{bd} did not yield any statistically significant differences, for both the x-axis ($F_{1.4,23.3} = 1.55, p = 0.23$) as well as the y-axis component ($F_{2,34} = 0.46, p = 0.64$). In opposition to Scenario 1 responsiveness of UAVs along the y-axis is lower than the one on the x-axis. The reason is that the obstacles block the movement along the y-axis.

V. DISCUSSION

The findings are consistent across the three maneuvering scenarios. First, haptic cues that are based on either *Veloc-*

[1] Bonferroni corrected i.e., $\alpha = 0.017$.

[2] Greenhouse-Geisser corrected.

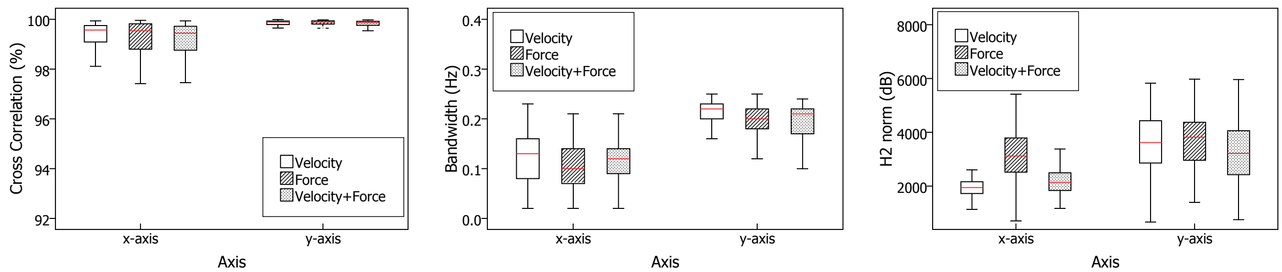

(a) (b) (c)

Fig. 5. Maneuverability performance in the Scenario 1. Boxplots indicate lower quartile, median and upper quartile. Whiskers represent the range of data: (a) Cross correlation of the position tracking, $CC_{position}(\%)$. (b) Bandwidth of the maneuverability, ω_{bd}. (c) H_2 norm of the maneuverability, $\|\Phi_{maneuv}\|_2$.

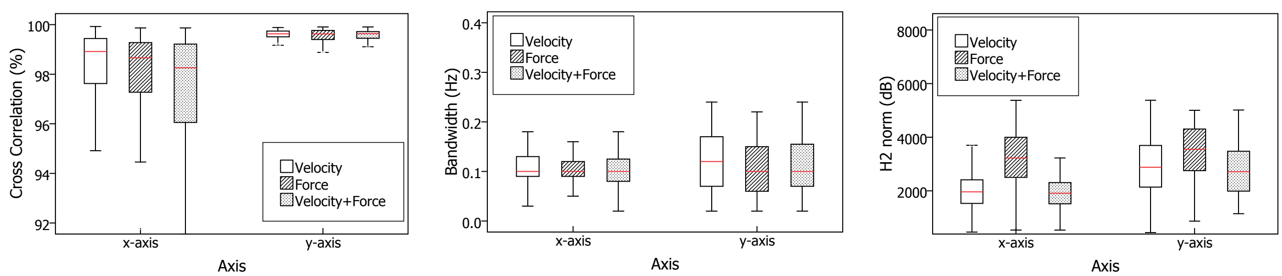

(a) (b) (c)

Fig. 6. Maneuverability performance in the Scenario 2. Boxplots indicate lower quartile, median and upper quartile. Whiskers represent the range of data: (a) $CC_{position}(\%)$. (b) ω_{bd}. (c) $\|\Phi_{maneuv}\|_2$.

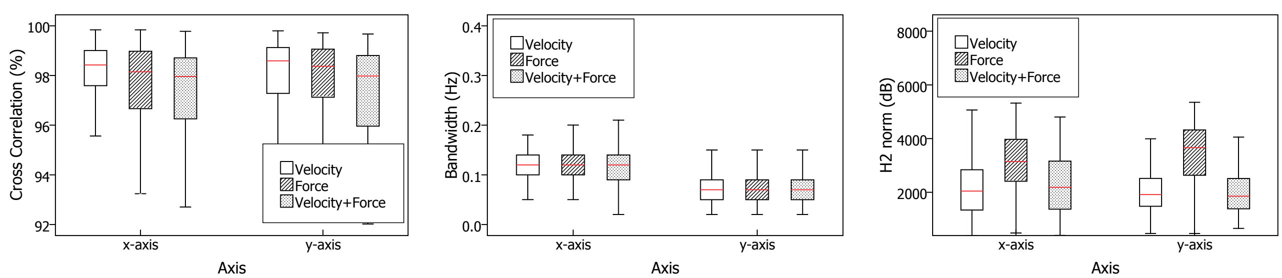

(a) (b) (c)

Fig. 7. Maneuverability performance in the Scenario 3. Boxplots indicate lower quartile, median and upper quartile. Whiskers represent the range of data: (a) $CC_{position}(\%)$. (b) ω_{bd}. (c) $\|\Phi_{maneuv}\|_2$.

ity or *Force* algorithms yield better tracking performance, relative to one that is based on a *Velocity+Force* algorithm, in situations that require obstacle avoidance (i.e., Scenario 2 and 3). Next, differences in the H_2 norm of our participants' frequency response suggest that a *Force* algorithm induces better maneuverability performance, relative to both *Velocity* and *Velocity+Force* algorithms (Scenarios 1, 2 and 3). This is because *Force* cues afford greater sensitivity in the transfer from the input force to tracking accuracy. In other words, less control effort is required on the part of the operator in achieving the same level of tracking accuracy with *Force* cues. One of the reasons is that, while the *force* cue is absent in free motion, the *Velocity* cue is absent only when UAVs move with a constant velocity vector, which is practically never the case. Therefore, in this case the user has always to counterbalance the inertia in order to obtain the desired motion.

It is worthwhile to note that there were no differences across the three types of haptic cues with respect to their performance bandwidth. Thus, the different algorithms did not appear to affect the accuracy in which the system tracked the operator's intended input.

In sum, our study demonstrates that a richer comparison of haptic feedback algorithms can be obtained by considering the frequency response profile of the human operator's force.

The current findings suggest that the *Force* cue is generally ideal for the control of multi-UAV systems. However, the suitability of haptic cue feedback might depend on the specific task that the tele-operator intends to achieve with the multi-UAV system. In our previous study, the *Velocity* cue was shown to be better than the *Force* cue in supporting the operator's ability to discriminate between the resistance of proximal obstacles, when participants' used the multi-UAV system to probe for invisible obstacles [10]. Maneuverability performance as well as perceptual awareness are equally important qualities during bilateral teleoperation. In light of this, the selection of haptic feedback algorithms ought to be weighted according to the application and the objective of the operator.

The feedback force to the human depends on the control parameters K and B in (10), (12), and (14). In the current study, the settings of these control parameters were pre-defined, according to our previous study [10], in order to produce the same magnitude of force for only *Velocity* and *Force* cue algorithms. We are conducting ongoing research that will define the functional relationship between the human force input and these control parameters, so as to allow for stronger generalizations of our present findings.

VI. CONCLUSION

In this paper, we propose performance metrics for maneuvering multi-robot systems which take into account the human operator's control effort during bilateral teleoperation. This contrasts with similar work that have tended to measure maneuverability solely in terms of position tracking accuracy (e.g., [14], [15]). Using our approach, we were able to assess the suitability of three haptic feedback algorithms in terms of how well they supported maneuverability performance in the haptic teleoperation of multiple UAVs; these algorithms were based on the UAVs' 1) velocity information, 2) obstacle avoidance force, and 3) the combination of these two information as the haptic cue. The results of our evaluation showed that the haptic feedback algorithm using the *Force* cue was the best in the maneuverability for all experimental scenarios with the statistical significance.

To conclude, maneuvering performance can be effectively evaluated in terms of the operator's frequency response, of the control input and desired output. This need not be restricted to the force input of the motor command. Other factors that are relevant to maneuvering performance could be similarly considered in like terms, such as design parameters of the haptic device and control parameters to evaluate the haptic device and the controller, respectively. Similarly, the desired output could be described in terms of other equally desirable objectives (e.g., the velocity and the force tracking), besides tracking accuracy (e.g., the system stability). Ultimately, the appeal of this approach lies in the fact that it allows performance of the human operator to be quantified in a manner that can be integrated into control systems, thus the system performance can be enhanced from the human perspective with an optimization in design and selection of the system parameters using the proposed metric and the psychophysical evaluation using it.

VII. ACKNOWLEDGMENTS

Research supported in part by the Max Planck Society and the WCU (World Class University) program through the National Research Foundation of Korea by the Ministry of Education, Science and Technology (R31-2008-000-10008-0).

REFERENCES

[1] R. Beckers, O. Holland, and J. Deneubourg, "From local actions to global tasks: Stigmergy and collective robotics," in *Artificial life IV: Proceedings of the Fourth International Workshop on the Synthesis and Simulation of Living Systems*, vol. 181, pp. 181–189, 1994.

[2] C. Jones, D. Shell, M. Mataric, and B. Gerkey, "Principled approaches to the design of multi-robot systems," in *Proceedings of the Workshop on Networked Robotics, IEEE/RSJ International Conference on Intelligent Robots and Systems*, 2004.

[3] R. Murray, "Recent research in cooperative control of multivehicle systems," *Journal of Dynamic Systems, Measurement, and Control*, vol. 129, no. 5, pp. 571–583, 2007.

[4] S. Sirouspour, "Modeling and control of cooperative teleoperation systems," *IEEE Transactions on Robotics*, vol. 21, no. 6, pp. 1220–1225, 2005.

[5] E. Rodriguez-Seda, J. Troy, C. Erignac, P. Murray, D. Stipanovic, and M. Spong, "Bilateral Teleoperation of Multiple Mobile Agents: Coordinated Motion and Collision Avoidance," *IEEE Transactions on Control Systems Technology*, vol. 18, no. 4, pp. 984–992, 2010.

[6] D. Lee, "Passive decomposition and control of nonholonomic mechanical systems," *IEEE Transactions on Robotics*, vol. 26, no. 6, pp. 978–992, 2010.

[7] K. P. Valavanis and K. P. Valavanis, *Advances in Unmanned Aerial Vehicles: State of the Art and the Road to Autonomy*. Springer Publishing Company, Incorporated, 2007.

[8] D. Lee, A. Franchi, P. Robuffo Giordano, H. I. Son, and H. H. Bülthoff, "Semi-autonomous haptic teleoperation of multiple unmanned aerial vehicles over the internet," in *Proceedings of the IEEE International Conference on Robotics and Automation*, pp. 1341–1347, May 2011.

[9] A. Franchi, P. Robuffo Giordano, C. Secchi, H. I. Son, , and H. H. Bülthoff, "A passivity-based decentralized approach for the bilateral teleoperation of a group of UAVs with switching topology," in *Proceedings of the IEEE International Conference on Robotics and Automation*, pp. 898–905, May 2011.

[10] H. I. Son, J. Kim, L. Chuang, A. Franchi, P. Robuffo Giordano, D. Lee, and H. H. Bülthoff, "An evaluation of haptic cues on the tele-operator's perceptual awareness of multiple UAVs' environments," in *Proceedings of the IEEE World Haptics Conference*, pp. 149–154, June 2011.

[11] J. McCarley and C. Wickens, "Human factors implications of UAVs in the national airspace," *Aviation Human Factors Division, Savoy, Illinois, Technical report AHFD-05-05/FAA-05-01*, 2005.

[12] N. Diolaiti and C. Melchiorri, "Teleoperation of a mobile robot through haptic feedback," in *IEEE International Workshop HAVE Haptic Virtual Environments and Their Applications*, pp. 67–72, 2002.

[13] K. Fite, L. Shao, and M. Goldfarb, "Loop shaping for transparency and stability robustness in bilateral telemanipulation," *IEEE Transactions on Robotics and Automation*, vol. 20, no. 3, pp. 620–624, 2004.

[14] I. Aliaga, A. Rubio, and E. Sanchez, "Experimental quantitative comparison of different control architectures for master-slave teleoperation," *IEEE Transactions on Control Systems Technology*, vol. 12, no. 1, pp. 2–11, 2004.

[15] Y. Yokokohji and T. Yoshikawa, "Bilateral control of master-slave manipulators for ideal kinesthetic coupling-formulation and experiment," *IEEE Transactions on Robotics and Automation*, vol. 10, no. 5, pp. 605–620, 1994.

[16] G. Burdea and M. Akay, *Force and touch feedback for virtual reality*. John Wiley & Sons New York, 1996.

[17] M.-D. Hua, T. Hamel, P. Morin, and C. Samson, "A control approach for thrust-propelled underactuated vehicles and its application to VTOL drones," *IEEE Transactions on Automatic Control*, vol. 54, no. 8, pp. 1837–1853, 2009.

[18] D. Lee and K. Huang, "Passive-set-position-modulation framework for interactive robotic systems," *IEEE Transactions on Robotics*, vol. 26, no. 2, pp. 354–369, 2010.

[19] K. Hashtrudi-Zaad and S. E. Salcudean, "Analysis of control architectures for teleoperation systems with impedance/admittance master and slave manipulators," *The International Journal of Robotics Research*, vol. 20, no. 6, pp. 419–445, 2001.

[20] L. Ljung, "On the estimation of transfer functions," *Automatica*, vol. 21, no. 6, pp. 677–696, 1985.